

## Journal Pre-proofs

### Original Article

A life cycle analysis on magnesium production processes: Energy consumption, carbon emission and economics

Xiaorui Huang, Zifu Xu, Liangliang Fu, Zhennan Han, Kun Zhao, Kangjun Wang, Dingrong Bai, Guangwen Xu

PII: S2588-9133(23)00073-X  
DOI: <https://doi.org/10.1016/j.crcon.2023.10.002>  
Reference: CRCON 202

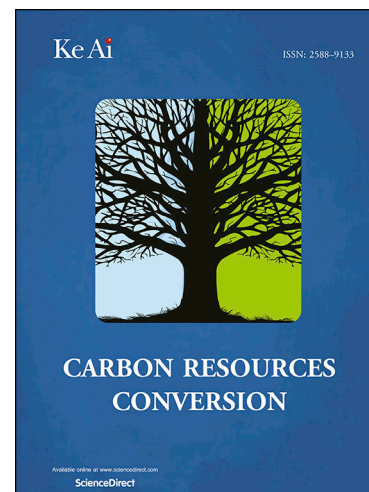
To appear in: *Carbon Resources Conversion*

Received Date: 18 July 2023  
Revised Date: 28 September 2023  
Accepted Date: 12 October 2023

Please cite this article as: X. Huang, Z. Xu, L. Fu, Z. Han, K. Zhao, K. Wang, D. Bai, G. Xu, A life cycle analysis on magnesium production processes: Energy consumption, carbon emission and economics, *Carbon Resources Conversion* (2023), doi: <https://doi.org/10.1016/j.crcon.2023.10.002>

This is a PDF file of an article that has undergone enhancements after acceptance, such as the addition of a cover page and metadata, and formatting for readability, but it is not yet the definitive version of record. This version will undergo additional copyediting, typesetting and review before it is published in its final form, but we are providing this version to give early visibility of the article. Please note that, during the production process, errors may be discovered which could affect the content, and all legal disclaimers that apply to the journal pertain.

© 2023 The Authors. Published by Elsevier B.V. on behalf of the National Institute of Oceanography and Fisheries.



# 1 **A Life Cycle Analysis on Magnesium Production Processes: Energy**

## 2 **Consumption, Carbon Emission and Economics**

3 Xiaorui Huang<sup>a,b</sup>, Zifu Xu<sup>a,b</sup>, Liangliang Fu<sup>a,b</sup>, Zhennan Han<sup>b</sup>, Kun Zhao<sup>b</sup>, Kangjun  
4 Wang<sup>b</sup>, Dingrong Bai<sup>b</sup>, Guangwen Xu<sup>a,b\*</sup>.

5 <sup>a</sup>University of Science and Technology Liaoning, School of Chemical Engineering,  
6 Anshan 114051, PR China

7 <sup>b</sup>Key Laboratory on Resources Chemicals and Materials of Ministry of Education,  
8 Shenyang University of Chemical Technology, Shenyang 110142, PR China

9

10 **Abstract:** Magnesium is widely used in manufacturing industry because of its excellent  
11 physical and chemical properties and has its increasing demand due to environmental  
12 requirements. China, as the world's biggest producer and exporter of metallic magnesium,  
13 produces metallic magnesium in its western provinces through the silico-thermic process  
14 known as the Pidgeon process. However, there are few metallic magnesium plants in  
15 eastern China, especially in Liaoning province where magnesite is rich in reserves. The  
16 short supply of magnesium has limited the growth of the magnesium casting industry and  
17 the local magnesite industry. Under the carbon market established to face the challenges  
18 of climate change, how to choose an economical and feasible route for magnesium  
19 production, is a key factor to determine the development of magnesium industry in  
20 Liaoning. In this paper, life cycle analysis models are developed to study the energy  
21 consumption, greenhouse gas (GHG) emissions, and economics from cradle to gate for  
22 six different metal magnesium production processes using data accounting for different  
23 geographical environments, process equipment, and energy supply pathways based on the  
24 Chinese Life Cycle Database (CLCD). The influence of carbon trading prices on  
25 economic performance of the six processes is also investigated. Compared with the  
26 current process widely used in China, the new magnesium production technology using  
27 Liaoning's abandoned magnesite as raw material and the coke oven gas from steelworks  
28 as fuel showed the best economic performance in terms of cost for greenhouse gas  
29 emissions.

30 **Keywords:** Magnesium, Pidgeon process, Thermal reduction, Life cycle, Greenhouse gas  
31 emission.

32

---

\* Corresponding author: Guangwen Xu. E-mail address: gw Xu@ipe.ac.cn

## 33 1. Introduction

34 Magnesium, a light silver-white alkaline earth metal and widely distributed in nature,  
35 has active chemical properties, certain ductility, and heat dissipation. It is the eighth-most  
36 abundant element in the earth's crust and the lightest structural metal [1]. During WWII,  
37 the magnesium industry grew rapidly, and the metal was widely used in fighter  
38 manufacturing in Germany because of its lightweight [2]. After the war, magnesium was  
39 gradually used in civilian applications [3], including the production of aluminum alloy,  
40 the production of magnesium alloy, titanium sponge, and steel desulfurization [4].  
41 Magnesium can also be used in rare earth alloys, metal reduction, corrosion protection,  
42 and other fields [5], [6]. The magnesium alloy features low density, high specific strength,  
43 high shock and dent resistance [7], [8], and thus has been widely used in 3C consumption,  
44 electronic industry, medical care, military projects, aviation, rail transit, and automobiles  
45 [9]–[11]. In particular, the application of magnesium alloys in vehicles attracted much  
46 attention due to the need for lightweight vehicles. Because of the low-density  
47 characteristic of magnesium alloy, the introduction of magnesium alloy into automobiles  
48 can effectively reduce the energy consumption and greenhouse gas emissions [12], [13].  
49 However, the metallic magnesium production process in China has been criticized for its  
50 high environmental burden [4].

51 There are two main ways to produce magnesium in industry, i.e., electrolysis and  
52 silicon thermal reduction [14]. According to the process characteristics, the silicon thermal  
53 reduction method has three alternatives: the Pidgeon process, the Bolzano process, and  
54 the Magnetherm process [4], [15]. Among these processes, the Pidgeon process which was  
55 invented by Dr. Pidgeon in the early 1940s [16] is the simplest, with less investment, and  
56 has been widely developed in China since 1988 [17]. The Pidgeon process had been  
57 applied in nearly all the Mg production plants in China. China is now the world's biggest  
58 producer of magnesium, almost all of which is produced using the Pidgeon process. In  
59 2018, global magnesium production reached 970k tons, of which 82.5% was contributed  
60 by China (MIIT, PRC, 2019). In China, the Pidgeon process operates in batch mode at  
61 elevated temperatures (about 1200 °C) and extract magnesium in the form of vapour from  
62 dolime ( $\text{MgO}\cdot\text{CaO}$ ) by a silico-thermic reduction reaction under a vacuum condition in  
63 an externally heated retort. Commonly, the dolomite is crushed into small pieces and then  
64 calcined in a rotary kiln at 1100-1300 °C for several hours to form dolime. Both  
65 silicothermic reduction and the carbonate decomposition are endothermic reactions, so  
66 the energy consumption of magnesium production is very high. A large amount of GHG  
67 emissions are emitted because the fossil fuels are used in the calcination and reduction  
68 stages of magnesium production [18]. These environmental problems have seriously  
69 limited the development of China's metallurgical magnesium production under the  
70 pressure of climate change and the China's carbon-neutral target. In 2020, the Ministry  
71 of Industry and Information Technology of China issued specifications and conditions for  
72 the magnesium industry, which set strict limits on energy consumption, equipment, and  
73 resource utilization rates for the magnesium industry, to change the current situation of  
74 high energy consumption and high pollution.

75 To solve the problem of energy conservation and GHG emissions in metallic  
76 magnesium production, we developed a number of magnesium production processes  
77 using fluidized bed technology. In these processes, the thermal decomposition of the  
78 carbonate occurs in a transport fluidized bed rather than in a conventional rotary kiln. In  
79 a transport fluidized bed, the raw material is ground into fine particles to achieve the  
80 fluidization. Compared with rotary kiln, transport fluidized bed can decompose carbonate  
81 in a few seconds at lower temperature due to reduced particle size and the improved heat  
82 transfer efficiency, thus reducing the energy consumption and GHG emissions [19]. In  
83 addition to dolomite, a low-rank magnesite from Liaoning province is also considered to  
84 be an ideal Mg resource due to its high Mg content and zero cost. Besides the traditional  
85 ferrosilicon reductant, aluminum is used as the reductant too because of the high  
86 magnesium yield by the alumino-thermic process during the reduction stage (Deng et al.,  
87 2014). In addition, the environmental burden of the process is also affected by the fuel  
88 selection strategies. Based on transport fluidized bed technologies, five different metallic  
89 magnesium production processes have been established considering different  
90 geographical environments, magnesium sources, reductants, and energy supply pathways.  
91 It's essential and necessary to comprehensively evaluate these five alternatives in order  
92 to determine whether the alternative processes are really energy efficient and environment  
93 friendly, so as to select the best process while the economic performance can not be  
94 neglected.

95 Life cycle assessment (LCA) is a holistic and powerful method for analyzing the  
96 environmental impacts of technology process, activity, or product during their life cycle  
97 [22], [23]. LCA is an appropriate approach, which takes into account different emissions  
98 of all materials and processes and provides a vital guidance for improving the  
99 performance from the environmental point of view through evaluating energy flow  
100 extensively [24]–[26]. Over the years, researchers have used LCA to investigate the  
101 environmental impacts from primary magnesium production [4], [27]–[31]. S and P  
102 [28] compared the emission of kg CO<sub>2</sub>-eq per unit weight of magnesium ingots produced  
103 by electrolysis and Pidgeon processes. Cherubini et al. [4] conducted a life cycle analysis  
104 of carbon emission for different magnesium production routes. Gao et al. [27] assessed  
105 the GHG emissions for the Pidgeon process and compared three scenarios with different  
106 fuels as energy sources.

107 The “cradle to gate” life cycle assessment is therefore used to focus on the economic,  
108 energy and environmental aspects of these five metallic magnesium production processes  
109 and the Pidgeon process. The first objective of this paper is to compare the Pidgeon  
110 process with alternative processes evaluated by LCA and to determine which process is  
111 the most environment-friendly and cost-saving, so as to provide a reference for upgrading  
112 the metallic magnesium production industry. The second objective is to establish a life  
113 cycle mode of the current Pidgeon process in China based on the Chinese life cycle  
114 database (CLCD) completely, which can be used for future related research and upgrade  
115 of the basic LCA database. This work is aimed at providing useful insight for the  
116 sustainable development of magnesium industries and the proper route selection.

117

## 118 **2. Methodology**

119 Fugu County, located in Shaanxi Province of China, is an essential magnesium  
120 smelting base and the largest industrial cluster of magnesium smelting enterprises in  
121 China and even the world. In 2019, Fugu's magnesium production accounted for more  
122 than 50% in China and 40% in the world. The production technology adopted in Fugu  
123 can be considered the most representative in magnesium production globally. For this  
124 reason, we chose the Pidgeon process used in Fugu as our research object and developed  
125 a life cycle model to assess the Pidgeon process based on the actual process data provided  
126 by the local authorities. The data was obtained by averaging the actual production data of  
127 a number of enterprises under the jurisdiction of the local authorities. Then, we  
128 established the life cycle assessment models for the other five alternative processes with  
129 reference to the Pidgeon process model according to the energy-material flow and energy-  
130 material conservation principle. The six models were computed by eFootprint, an online  
131 life cycle assessment platform based on the CLCD. From the results, the energy  
132 consumption, carbon emission, and economics of the life cycle magnesium production  
133 processed can be evaluated quantitatively and precisely.

134 In this work, we followed the ISO guidelines, which consist of four steps: goal and  
135 scope definition, life cycle inventory (LCI), life cycle impact assessment (LCIA), and  
136 interpretation.

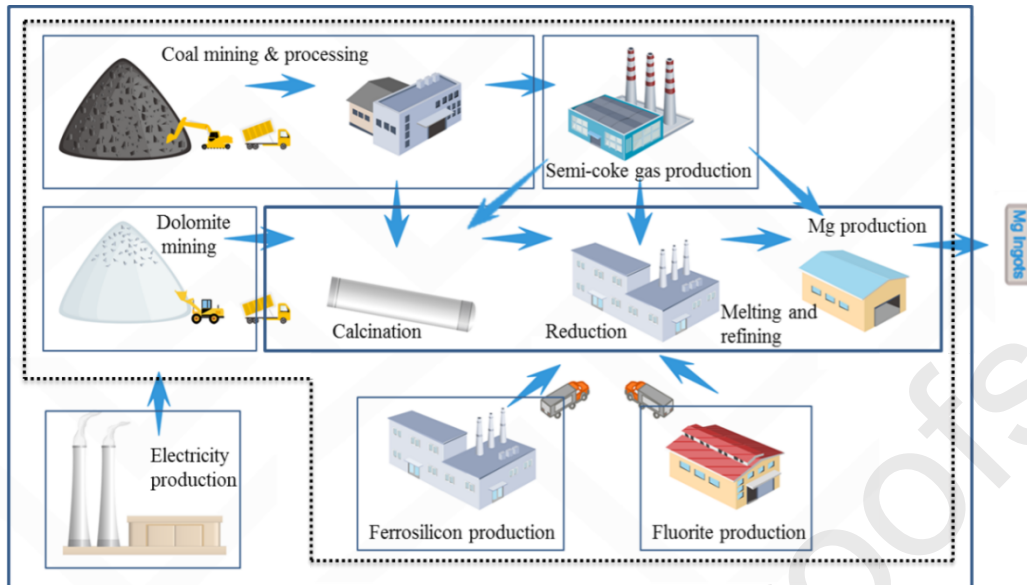
### 137 ***2.1. Goal and scope definition***

138 The goal of this work is to evaluate the environmental and economic impacts of the  
139 Pidgeon process and other five alternatives for the production of primary magnesium in  
140 order to assess the environmental and economic feasibility of alternative processes. The  
141 assessment system boundaries of all the six processes are defined as “cradle to gate”,  
142 including all the phases involved from mining of raw materials to final products.

143 The assessment system includes raw ores mining, transportation, reductant  
144 production, primary magnesium production, fuel production and all the auxiliary systems  
145 related to environmental impacts, such as power generation and coal mining & processing.  
146 The functional unit is the production of 1 tone of Mg ingots in this study.

### 147 ***2.2. Scope of Pidgeon process***

148 The life cycle of Pidgeon process in Fugu, shown in Fig. 1, includes eight stages:  
149 transportation, coal mining & processing, semi-coke gas production, dolomite mining,  
150 ferrosilicon production, fluorite production, Mg production and electricity production.



151

152

Fig. 1. Life cycle of Mg ingots production in Fugu.

153

154

155

156

157

158

159

160

161

162

163

**Transportation.** All the transportation activities within the system scope were included. But only long-distance transportation is considered while transportation between the production departments is ignored in the analysis. Dolomite ore and ferrosilicon are trucked from neighboring Shanxi province to the calcination and reduction departments of the Mg plant, respectively, with an average distance of 50 km. Fluorite ore is delivered by truck an average of 100 km from Inner Mongolia to the reduction department of the Mg plant. The coal plant and the Mg plant are close, so the transportation between them is ignored. The semi-coke gas is piped a short distance to the reduction department, and the washed coal is sent to the plant on belt conveyors, so the transportation of semi-coke gas and washed coal is omitted too. All the road transportation is fueled with diesel.

164

165

166

**Coal mining and processing.** Raw coal is mined and transported to the coal washing plant, where it is washed according to the quality requirements. On average, 1.21 ton of raw coal produces 1 ton of washed coal with an consumption of 7.27 kWh of electricity.

167

168

169

170

171

172

173

174

175

**Semi-coke gas production.** The washed coal is fed into a coke oven to produce semi-coke and semi-coke gas. In this process, the production of 1.0t semi-coke, 0.101t coal tar and 1.479t semi-coke gas consumes 1.65t washed coal, 125 kWh electricity and 0.594t semi-coke gas. The semi-coke gas is cooled and purified, and is further used as fuel for reduction, melting and refining in the magnesium plant. The semi-coke gas production is a multi-output system, and the allocation of energy consumption and emission in the system are considered in order to determine the environmental effect of semi-coke gas precisely. With the mass allocation method, the allocation factors of the semi-coke and the semi-coke gas are calculated as 38.76% and 57.33%, respectively.

176

**Dolomite mining.** Dolomite ore is the principal raw material, mined and transported

177 to the Mg plant. It takes 11 tons of ore to produce 1 ton of Mg.

178 **Ferrosilicon production.** The ferrosilicon, containing 75% silicon and 25% iron, is  
179 used as the reductant in the reduction process. Ferrosilicon is produced in three-phase  
180 submerged arc furnaces by the carbo-thermic reduction of silica in the presence of high-  
181 quality scrap steel with an extensive power consumption. 1.06 tons of ferrosilicon is  
182 needed to produce 1 ton of Mg.

183 **Fluorite production.** Fluorite is mined and transported to the Mg plant. 0.15 tons of  
184 fluorite is need to produce 1 ton of Mg.

185 **Mg production.** The dolomite is calcined in a rotary kiln at a high temperature  
186 ranging from 1150 to 1250 °C. The major ingredient  $\text{CaCO}_3 \cdot \text{MgCO}_3$  is decomposed  
187 into MgO and CaO (i.e. dolime), and  $\text{CO}_2$  is released during the calcination process.  
188 Semi-coke gas and coal powder are used as fuel for calcining dolomite. The dolime,  
189 ferrosilicon, and fluorite are grounded separately and mixed in specific proportion. The  
190 mixture is pressed into briquettes and used as the feedstock for the reduction process.  
191 They are fed into the horizontal pots in a furnace heated externally by the semi-coke gas  
192 at a temperature of about 1200 °C and a vacuum pressure of 10 Pa. The magnesium is  
193 reduced to vapor which is condensed into crown crystal on the recyclable water-cooled  
194 head of the pot. The crown magnesium obtained from the reduction process is then melted  
195 in a melting furnace and refined by heating the melt above the melting point of 740 °C.  
196 Finally, the molten magnesium is cast into magnesium ingots. The semi-coke gas was  
197 used as the fuel in this refining process.

198 **Electricity production.** Electricity is taken from the Northwest China power grid  
199 and transmitted to the magnesium plant.

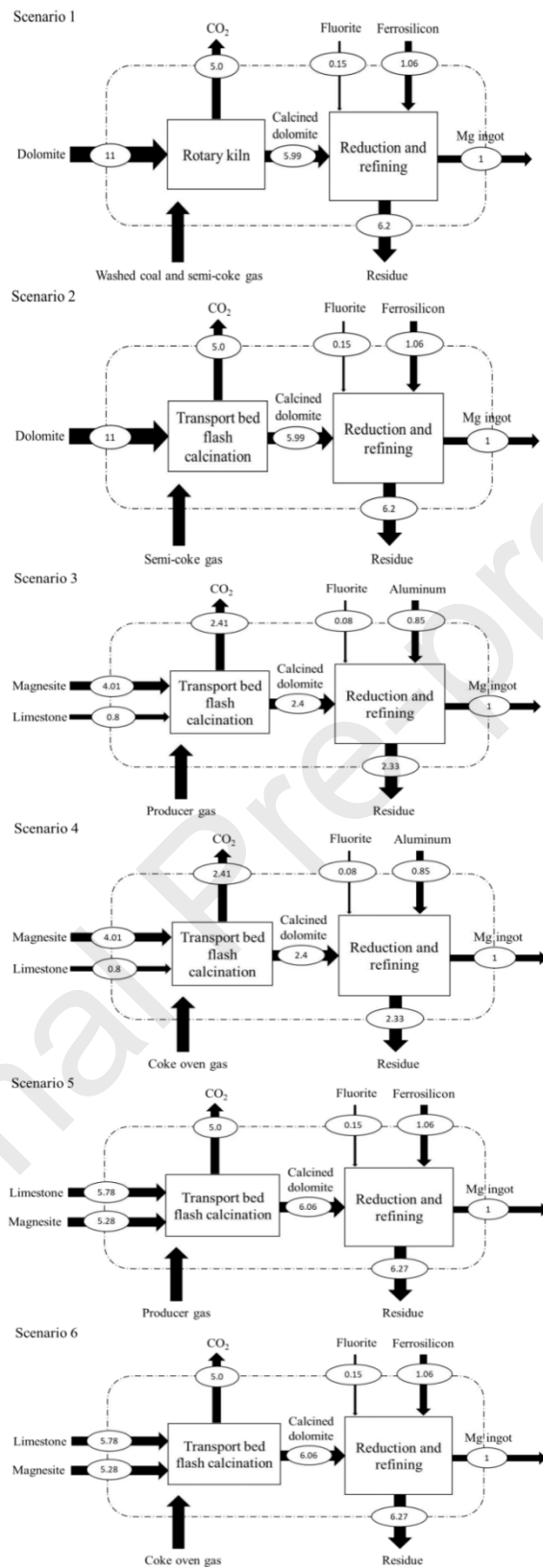
### 200 **2.3. Description of Mg production processes scenarios**

201 Currently, the Mg can be produced by several alternative processes, although the  
202 Pidgeon process is mainly employed in China. In order to gain insights into improving  
203 the performance of Mg production, all these alternative processes are evaluated in this  
204 study on the basis of the same conditions of Pidgeon process, as shown in Fig. 2. In  
205 these processes, combined with the actual situation in Liaoning, three strategies for  
206 energy saving and  $\text{CO}_2$  reduction are introduced, including the selection of reducing  
207 agents, the upgrading of calcination equipment, and the change of fuel gas.

208 The differences among the six Mg production processes scenarios are mainly in the  
209 stage of Mg production. Scenario 1 is the Pidgeon process and has been previously  
210 discussed. Scenario 2 introduces a transport fluidized bed to calcine dolomite rather than  
211 the traditional rotary kiln. In scenario 3, the limestone and magnesite ores are used as the  
212 raw materials to produce Mg with aluminum reductant [32], [33]. Aluminum of 99% purity  
213 is used as the reductant and 2 wt%  $\text{CaF}_2$  is added. Magnesite with 46 wt% MgO and  
214 limestone (52 wt% CaO) are the resource of magnesium. The transport fluidized bed is  
215 used as calcination equipment and the producer gas is used as fuel gas. Scenario 4, based

216 on Scenario 3, uses the coke oven gas from the steelworks as fuel. In scenario 5, the  
217 transport fluidized bed is used to calcinate the raw ore particles. Grade 3 magnesite (43  
218 wt% MgO), normally discarded as solid waste in Liaoning, and limestone (52 wt% CaO)  
219 are used as feedstocks to produce dolime during the calcination stage. Producer gas was  
220 used as fuel gas. Scenario 6, based on scenario 5, uses coke oven gas for the energy supply  
221 of the system. It is worth noting that scenario 3, 4, 5, and 6 are suitable for Liaoning  
222 province due to its extremely rich magnesite resources.





223

224 Fig. 2. System boundaries and mass flow of six Mg ingot production scenarios (unit:  
 225 t).

226 **2.4. Life cycle inventory (LCI)**

227 The foreground data of raw materials and energy inputs in scenario 1 comes from  
 228 Fugu authorities (Shaanxi, China), representing the average production level of local Mg  
 229 plants. The foreground data of raw materials and energy consumption in other scenarios  
 230 are calculated based on the principles of conservation of mass and energy using the  
 231 relevant data from published studies, patents, and comparisons with the silicon-thermic  
 232 process [34], [35]. The detailed data is presented in Fig. 2 and Table 1. The background  
 233 data is retrieved from the China life cycle database (CLCD) in the software ebalance.  
 234 Transportation for all scenarios is determined by the location of the source of raw  
 235 materials and fuel. Electricity consumption in all the scenarios is assumed to be the same,  
 236 since electricity is consumed primarily for utilities.

237 Table 1. LCI of Mg production scenarios for 1 tone Mg ingot.

Item	Unit/tonnes <sub>Mg</sub>	Scenarios					
		S1	S2	S3	S4	S5	S6
Mg ingots production							
Dolomite	tonnes	11	11				
Limestone				0.8	0.8	5.78	5.78
Magnesite	tonnes			4.01	4.01	5.28	5.28
Ferrosilicon	tonnes	1.06	1.06			1.06	1.06
Aluminum	tonnes			0.85	0.85		
Fluorite	tonnes	0.15	0.15	0.08	0.08	0.15	0.15
Washed coal	tonnes	1.5					
Semi-coke gas	m <sup>3</sup>	16000	14308				
Producer gas	m <sup>3</sup>			12252		19547	

Coke oven gas	m <sup>3</sup>				4039		6444
Electricity	kWh				1200		
Road transportation	t·km	618	618	179	370	754	734
Railway transportation	t·km					1378	1336
Product							
Mg ingots	tonnes				1.00		

#### 238 2.4. Life cycle impact assessment (LCIA)

239 The LCIA is used for quantitative analysis of the possible environmental impacts,  
 240 such as resource and energy consumption, ecological damage, human health damage,  
 241 based on the life cycle inventory [36], [37]. The LCIA method adopted by eFootprint  
 242 platform is a comprehensive evaluation index based on the mid-point method according  
 243 to China's energy conservation and emission reduction policy objective [38]. The selected  
 244 mid-point categories are global warming potential (GWP, kg CO<sub>2</sub> eq.), primary energy  
 245 demand (PED, MJ), resource depletion-water (WU, kg), acidification (AP, kg SO<sub>2</sub> eq.),  
 246 abiotic depletion potential (ADP, kg Sb eq.), eutrophication (EP, kg PO<sub>4</sub><sup>3-</sup> eq.), particulate  
 247 matter (RI, kg PM<sub>2.5</sub> eq.), Ozone depletion (ODP, kg CFC-11 eq.), and photochemical  
 248 ozone formation (POFP, kg NMVOC eq.).

249 This study takes primary energy demand and global warming potential as  
 250 environmental indicators to evaluate energy consumption and greenhouse gas emissions  
 251 of the six scenarios. The results are calculated based on the background data of the  
 252 scenarios and the corresponding parameters in the CLCD. Note that the life cycle GHG  
 253 emissions released throughout the scenarios can be divided into direct carbon emissions  
 254 and indirect carbon emissions. The GHG emissions from the combustion of fuels and the  
 255 decomposition of raw carbonate ores belong to direct carbon emissions, while other GHG  
 256 emissions from the upstream processes are considered indirect carbon emissions.

257 The GHG emissions emitted from carbonate ores calcination are calculated by the  
 258 following equation.

$$259 \quad E_{DC} = M_1 \times \frac{44}{40} + M_2 \times \frac{44}{56}$$

260 Where  $M_1$  is the quantity of MgO,  $M_2$  is the quantity of CaO and  $E_{DC}$  represented GHG  
 261 emissions emitted from the dolomite calcination process.

262 The GHG emissions associated with fuel combustion are estimated by the following  
 263 equation.

$$264 \quad E_{FC} = \frac{44}{12}MQK\alpha$$

265 Where,  $E_{FC}$  is the GHG emission quantity from fuel combustion (kg CO<sub>2</sub> -eq),  $\frac{44}{12}$  is  
 266 the molecular mass ratio of carbon dioxide to carbon, M is the fuel consumption (kg), Q  
 267 is the calorific value of fuel (MJ/kg), K is the carbon emission coefficient of fuel  
 268 combustion (kg C/MJ) and  $\alpha$  is the carbon oxidation ration of fuel (%). The parameter  
 269 values of the washed coal are listed in Table 2. The GHG emissions of the fuel gases  
 270 combustion are calculated according to their composition, as shown in Table 3.

271 Table 2. The parameter values of washed coal.

Fuel	Q (MJ/kg)/( MJ/m <sup>3</sup> )	K (kg C/MJ)	$\alpha$ (%)
Washed coal	26.4	$25.8 \times 10^{-3}$	1

272 Data comes from IPCC 2006

273

274 Table 3. The characteristics of fuel gases.

Gas	Component (V %)							Calorific value (MJ/m <sup>3</sup> )
	H <sub>2</sub>	CH <sub>4</sub>	CO	N <sub>2</sub>	CO <sub>2</sub>	CmHn	O <sub>2</sub>	
Semi-coke gas	27	7.5	11.5	45.5	7.5	0.3	0.7	7.75
Coke oven gas	55	24	14.5		3.5	2.3	0.1	16.35
Producer gas	13	2.2	27.5	51.8	5	0.3	0.2	5.39

## 275 2.5. Production cost of Mg production

276 The total production costs include the cost of the raw ore (dolomite, magnesite, and  
 277 limestone), the catalyst (fluorite), the fuel (coal and fuel gasses), the reductant  
 278 (ferrosilicon and aluminum), the utilities (electricity), and the lost reduction pots. Mg  
 279 production cost are estimated based on raw material price in China in 2019 published by  
 280 Metal news, as shown in Table 4. Due to the limited material technology, the reduction  
 281 pot has a relatively short service life and is replaced frequently during the Mg production  
 282 period, so the cost of the reduction pot needs to be considered. Meanwhile, the impact of

283 GHG emissions on the economy is studied by monetizing GHG emissions in the carbon  
 284 trading markets in China and the European Union (EU).

285 Table 4. The raw material prices of Mg production.

Specie	List	Price
Raw ore	Dolomite	100 ¥/t
	Magnesite	10 -400 ¥/t
	Limestone	100 ¥/t
Catalyst	Fluorite	1800 ¥/t
Fuel	Washed coal	500 ¥/t
	Semi-coke gas	0
	Producer gas	0.28 ¥/m <sup>3</sup>
	Coke oven gas	0
Reductant	Ferrosilicon	5750 ¥/t
	Aluminum	14420 ¥/t
Power	Electricity	0.75¥/kWh
Equipment loss	Reduction pot	3600 ¥/t Pidgeon Mg
Carbon cost	CO <sub>2</sub> emissions	53 - 191 ¥/t CO <sub>2</sub> -eq

287 **3. Results and Discussion**288 **3.1. Analysis of LCA results in S1 (Pidgeon process)**

289 The calculated PED and GWP results of S1 are listed in Table 5. To examine the  
 290 individual contribution of each life cycle inventory of S1, the relative contribution (%) of  
 291 each item to the selected environmental impact categories is shown in Fig. 3.

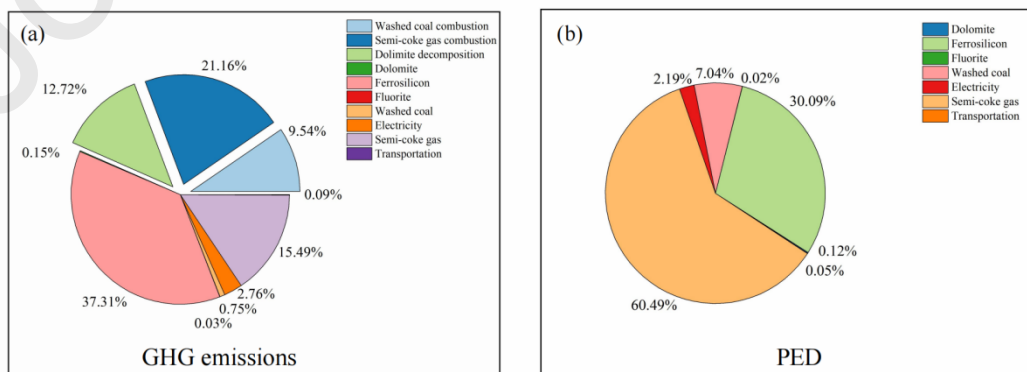
292 Table 5. Life cycle PED and GWP results of S1 (Pidgeon process).

Item	PED (MJ)	GWP (kg CO <sub>2</sub> eq.)
Dolomite	760	59.6
Ferrosilicon	1.92x10 <sup>5</sup>	1.47x10 <sup>4</sup>
Fluorite	139	10.4
Washed coal	4.49x10 <sup>4</sup>	296
Electricity	1.4x10 <sup>4</sup>	1.08x10 <sup>3</sup>
Semi-coke gas	3.86x10 <sup>5</sup>	6.09x10 <sup>3</sup>
Transportation	347	36
Washed coal combustion		3.75x10 <sup>3</sup>
Semi-coke gas combustion		8.32x10 <sup>3</sup>
Dolomite decomposition		5x10 <sup>3</sup>
		Direct emissions
		1.71x10 <sup>4</sup>
Total	6.38x10 <sup>5</sup>	3.93x10 <sup>4</sup>

293 It shows that for 1 ton Mg produced, the energy consumption and the GHG emissions  
 294 are 6.38x10<sup>5</sup> MJ and 3.93x10<sup>4</sup> kg CO<sub>2</sub>-eq., respectively. Ehrenberger Simone has  
 295 conducted a detailed carbon footprint study of magnesium and its application in

296 automobiles[30], [39]. Their work is greatly appreciated and serves as a guidance  
 297 document recommended by the International Magnesium Association. Based on their  
 298 research, from a cradle to gate perspective, the overall average emissions of the  
 299 magnesium production in China amount to 28 kg CO<sub>2</sub>-eq. per kg magnesium (including  
 300 all upstream processes) of which the carbon emissions of the semi-coke gas-fueled  
 301 process amount to about 19 kg CO<sub>2</sub>-eq. per kg magnesium. In their study, they suggested  
 302 that the semi-coke gas could be credited to the magnesium production system, as the gas  
 303 would be released into the atmosphere if not used, with a credit of about 9 kg CO<sub>2</sub>-eq. In  
 304 fact, due to the large-scale use of semi-coke gas in the magnesium production, the  
 305 production of semi-coke gas has become a matching process for the production of  
 306 magnesium, hence we do not credit semi-coke gas in this paper. In the Pidgeon process  
 307 without upstream processes, the carbon emissions result calculated by Ehrenberger  
 308 Simone is 12.1 kg CO<sub>2</sub>-eq, and our result is 17.1 kg CO<sub>2</sub>-eq. This is because the  
 309 magnesium enterprise in Fugu uses extra coal powder besides the semi-coke gas to  
 310 calcinate dolomite, which can be found in the life cycle list above. In addition, in the  
 311 production of ferrosilicon, Ehrenberger Simone considers a carbon emission of 12.5 kg  
 312 CO<sub>2</sub>-eq, whereas we consider it to be 14.7 kg CO<sub>2</sub>-eq. This is because Ehrenberger  
 313 Simone adopted the value of advanced ferrosilicon production processes, while we  
 314 adopted the average value of Chinese ferrosilicon enterprises. The remaining value  
 315 discrepancy is caused by the difference between the Ecoinvent database and the CLCD  
 316 used for the background data.

317 As shown in Fig 3(a), the combustion of washed coal and semi-coke gas contributes  
 318 30.70%, and the decomposition of dolomite 12.72% to the total GHG emissions. This  
 319 indicates that the carbon footprint of S1 comes mainly directly from the combustion of  
 320 fuel. The productions of ferrosilicon, semi-coke gas, and electricity emit indirectly 37.31  
 321 %, 15.4%, and 2.76%, respectively. The GHG emissions from dolomite, fluorite, washed  
 322 coal, and transportation are low and can be ignored. Regarding PED, it's found that the  
 323 ferrosilicon, the semi-coke gas, and washed coal are the main contributors, and the  
 324 contribution of dolomite, fluorite, and transportation could be ignored because of their  
 325 tiny shares (<1%), as shown in Fig. 3(b). It is apparent that energy-saving measures  
 326 should be taken in energy utilization and ferrosilicon production processes so that PED  
 327 can be effectively reduced.







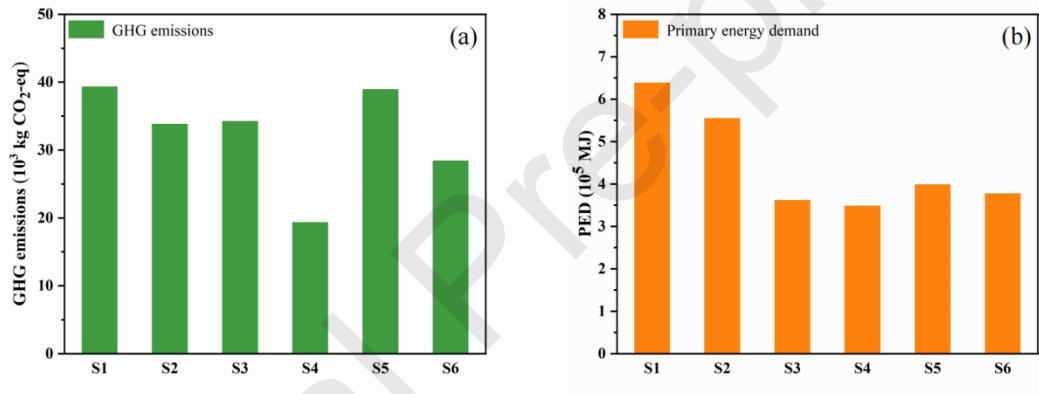
Transportation	Road	36	36	10.4	21.6	43.9	42.7
	Railway					14.1	13.7
Direct contribution	Carbonate decomposition	$5 \times 10^3$	$5 \times 10^3$	$2.41 \times 10^3$	$2.41 \times 10^3$	$5 \times 10^3$	$5 \times 10^3$
	Fuel combustion	$1.21 \times 10^4$	$7.45 \times 10^3$	$8.35 \times 10^3$	$3.51 \times 10^3$	$1.33 \times 10^4$	$5.61 \times 10^3$
	Total	$3.93 \times 10^4$	$3.38 \times 10^4$	$3.42 \times 10^4$	$2.76 \times 10^4$	$3.89 \times 10^4$	$2.84 \times 10^4$

338  
339

Table 7. Comparative analysis of the six metallic magnesium production scenarios in primary energy demand.

Item	PED (MJ)					
	S1	S2	S3	S4	S5	S6
Dolomite	760	760				
Carbonate ore	Magnesite		277	277	365	365
	Lime		55.3	55.3	399	399
	Ferrosilicon	$1.92 \times 10^5$	$1.92 \times 10^5$			$1.92 \times 10^5$
Reductant	Aluminum		$2.27 \times 10^5$	$2.27 \times 10^5$		
	Fluorite	139	139	74.2	74.2	139
Fuel	Washed coal	$4.49 \times 10^4$				
	Coke oven gas				$1.06 \times 10^5$	$1.7 \times 10^5$

	Producer gas			$1.19 \times 10^5$		$1.9 \times 10^5$	
	Semi-coke gas	$3.86 \times 10^5$	$3.47 \times 10^5$				
	Electricity	$1.4 \times 10^4$	$1.4 \times 10^4$	$1.4 \times 10^4$	$1.4 \times 10^4$	$1.4 \times 10^4$	$1.4 \times 10^4$
Transportation	Road	347	347	101	208	423	412
	Railway					176	170
	Total	$6.38 \times 10^5$	$5.54 \times 10^5$	$3.61 \times 10^5$	$3.48 \times 10^5$	$3.98 \times 10^5$	$3.77 \times 10^5$



340

341

Fig. 4. GWP (a) and PED (b) results of the six scenarios.

342

343

344

345

For the six metallic magnesium production scenarios, carbon emissions are dominated by carbonate ore decomposition, fuel combustion, and the preparation of reductant. The energy is mainly consumed in the productions of reductant, fuels, and electricity in these six scenarios.

346

347

348

349

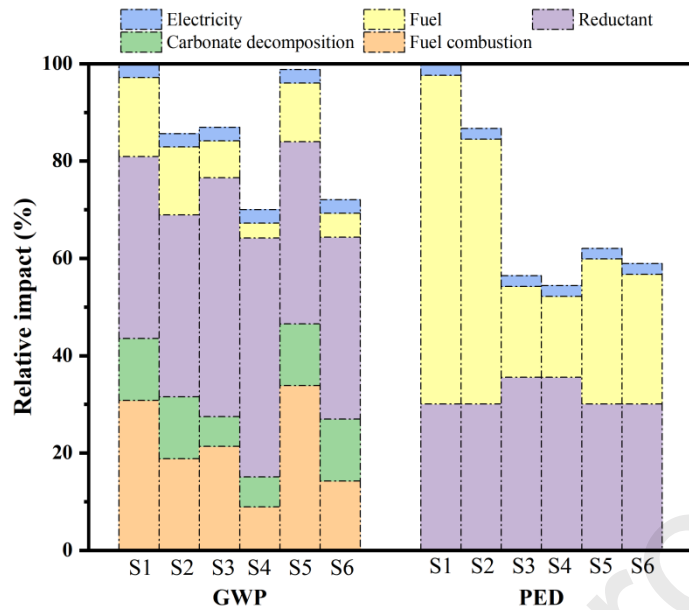
350

351

352

353

It can be seen that to produce 1 ton Mg product, the process order in terms of GWP is as follow: S1 ( $3.93 \times 10^4 \text{ kg CO}_2\text{-eq}$ ) > S5 ( $3.89 \times 10^4 \text{ kg CO}_2\text{-eq}$ ) > S3 ( $3.42 \times 10^4 \text{ kg CO}_2\text{-eq}$ ) > S2 ( $3.38 \times 10^4 \text{ kg CO}_2\text{-eq}$ ) > S6 ( $2.84 \times 10^4 \text{ kg CO}_2\text{-eq}$ ) > S4 ( $2.76 \times 10^4 \text{ kg CO}_2\text{-eq}$ ). In terms of energy consumption, the order is S1 ( $6.38 \times 10^5 \text{ MJ}$ ) > S2 ( $5.54 \times 10^5 \text{ MJ}$ ) > S5 ( $3.98 \times 10^5 \text{ MJ}$ ) > S6 ( $3.77 \times 10^5 \text{ MJ}$ ) > S3 ( $3.61 \times 10^5 \text{ MJ}$ ) > S4 ( $3.48 \times 10^5 \text{ MJ}$ ). It indicates that S4 has the lowest energy consumption and carbon emissions for the production of Mg. It shows that S1 and S5 are close in GHG emissions, but S1 consumes significantly greater energy than S5.



354

355 Fig. 5. Comparative GHG emissions and PED results for the six scenarios (Note: in the  
 356 figure, the highest impact was defined as 100%, and each bar represented the relative  
 357 percent to the highest score).

358 In order to further identify the share of each life cycle inventory to the overall GWP  
 359 and PED of the six scenarios, the contribution (%) of each item is estimated as shown in  
 360 Fig. 5. For all these scenarios, the raw ores, fluorite production, and transportation  
 361 contribute little to the GWP and PED, and are neglected. For GHG emissions, the impacts  
 362 of six scenarios are 100%, 85.64%, 86.90%, 70.00%, 98.77%, and 72.03%, respectively.  
 363 And for PED, the impacts of the six scenarios is 100%, 86.67%, 56.42%, 54.38, 62.06%  
 364 and 58.93%, respectively.

365 The reason why the energy consumption of S2 is 86.67% of that of S1 is that the  
 366 energy consumption of fuel production of S2 is 13.15% less than that of fuel production  
 367 of S1. Due to the high thermal efficiency calcination technology based on fluidized bed,  
 368 the calcination stage of the feedstock in S2 requires less heat than that in S1 and can be  
 369 completely supplied by gaseous fuel. The reduction in fuel consumption directly leads to  
 370 a reduction in GHG emissions during fuel combustion, as well as a reduction in GHG  
 371 emissions during fuel production. As a result, the greenhouse gas emissions from fuel  
 372 combustion in S2 are 11.96% less than those in S1, and the greenhouse gas emissions  
 373 from fuel production in S2 are 2.31% less than those in S1. This makes GHG emissions  
 374 of S1 86.67% of that of S1.

375 The comparison of the PED results between S3 and S2 shows that the energy  
 376 consumption of the reductant production in S3 is 5.49% higher than that in S2, since the  
 377 energy consumption of aluminum production is higher than that of ferrosilicon production.  
 378 However, the energy consumption required for fuel production is 35.74% less than that  
 379 of S2. This is due to the high reduction efficiency of aluminum as reductant, which

380 requires less fuel to produce the same weight of the products. Thus, the total energy  
381 consumption of S3 is 30.25% less than that of S2. Compared to the GWP results of S2,  
382 the greenhouse gasses from fuel production and carbonate decomposition in S3 are 6.38%  
383 and 6.59% less than those in S2, respectively, because the efficient thermite reduction  
384 reduces not only fuel consumption but also carbonate feedstock consumption. As for the  
385 greenhouse gas emissions generated in the production of the reductant, the emission in  
386 S3 is 11.71% higher than that in S2. This is because aluminum is prepared from the  
387 electrolysis process, and the electricity is mainly generated by coal-fired power plants,  
388 which results in GHG emissions. The greenhouse gas emissions from fuel combustion in  
389 S3 are 2.52% higher than that in S2 because the carbon content of the producer gas is  
390 greater than that of the semi-coke gas, as shown in Table 2. The carbon emission of S3 is  
391 1.26% higher than that of S2 due to the contribution of reductant and fuel combustion to  
392 the GWP of S3.

393 The difference in the PED results between S3 and S4 is because of the different  
394 energy consumption required for fuel production. The difference is small, only 2.04%,  
395 suggesting that the energy consumption required to produce a unit of heat value for the  
396 producer gas and the coke oven gas is similar from LCA perspective. The difference in  
397 the GWP results between S3 and S4 is caused by the difference in the greenhouse gasses  
398 emitted during fuel production and combustion. Compared to S3, carbon emissions from  
399 fuel combustion and fuel production in S4 are reduced by 12.42% and 4.48% respectively,  
400 resulting in 16.9% of the total reduction in carbon emissions. This is because the  
401 production of coke oven gas emits fewer greenhouse gasses per unit heat value than the  
402 production of producer gas, and the carbon content of coke oven gas is much smaller than  
403 that of producer gas, as shown in Table 2. It indicates that the coke oven gas is more  
404 suitable as a fuel than producer gas considering GHG emissions and PED in LCA view.

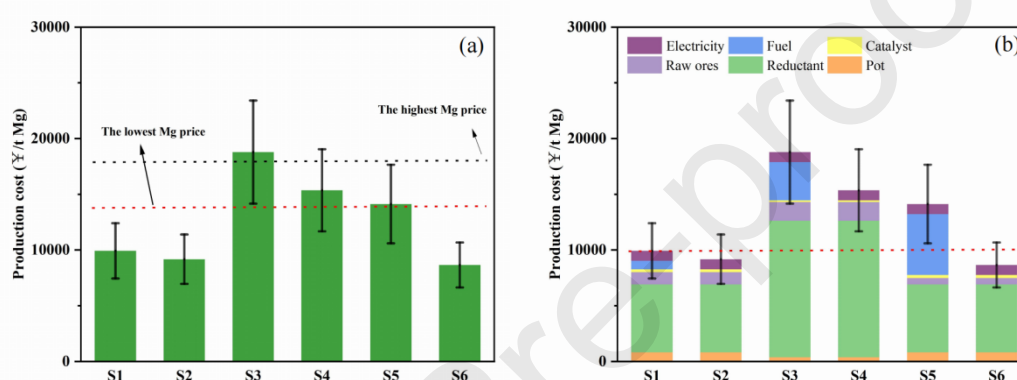
405 Thanks to the difference in energy consumption required for fuel production, the  
406 energy consumption of S5 is 24.61% less than that of S2. However, the GWP of S5 is  
407 13.13% higher than that of S2. This is because the greenhouse gas emissions from fuel  
408 combustion in S5 are 15.01% more than S2, while the greenhouse gas emissions from  
409 fuel production are 1.88% less than S2. From the point of view of the LCA, the energy  
410 consumption and greenhouse gas emission of producer gas per calorific value are less  
411 than that of semi-coke gas, but the carbon content of producer gas is more than that of  
412 semi-coke gas, and therefore its carbon emissions are higher than those of semi-coke gas.

413 The energy consumption of S6 is only 3.13% lower than that of S5, but the carbon  
414 emissions of S6 are 26.74% lower than those of S5, due to the use of coke oven gas as  
415 fuel. The energy consumption of reductant production in S6 is 5.49% lower than that of  
416 S4, and the energy consumption of fuel production is 10.04% higher than that of S4,  
417 resulting in a 4.55% of total energy consumption increase in S6. This is because  
418 aluminum production requires higher energy consumption than ferrosilicon production,  
419 but the introduction of aluminum reductant makes the energy consumption of magnesium  
420 production per unit weight much lower than ferrosilicon reductant. In the comparison of  
421 the GWP results between S6 and S4, the GHG emissions from fuel combustion, carbonate

422 decomposition, and fuel production in S4 are reduced by 5.32%, 6.59%, and 1.83%,  
 423 respectively. However, the carbon emissions from the reductant production in S4 are  
 424 increased by 11.71%, which makes the carbon emissions in S4 only 2.03% less than those  
 425 in S6. This is also because a large amount of greenhouse gases are emitted during the  
 426 process of aluminum production.

### 427 3.3. Economic performance

428 The production costs of the six scenarios are shown in Fig. 6, in which each bar  
 429 represents the average value, and the error lines on each bar represent the range of the Mg  
 430 ingot cost according to 25% price fluctuation of the corresponding raw materials and  
 431 energy.



432  
433 Fig. 6. Production costs of the six scenarios.

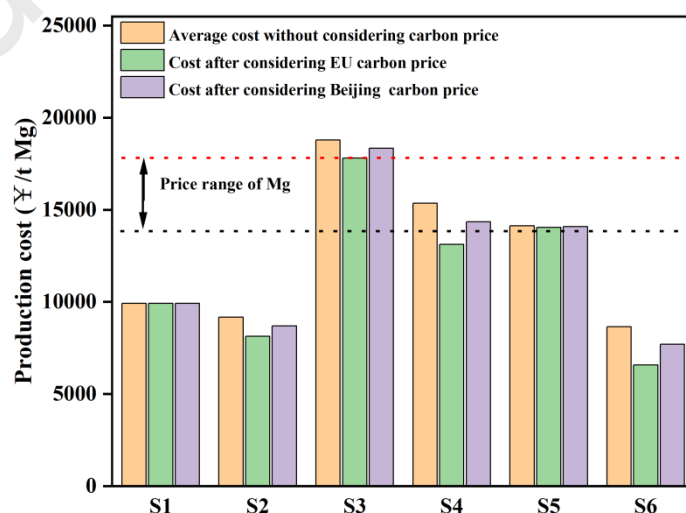
434 It can be seen that the average production cost ranges from about 8653 to 18790 ¥/t,  
 435 with S6 being the lowest and S3 being the highest, as shown in Fig. 6(a). For S1, S2, S4,  
 436 S5 and S6, the average production costs are 9925, 9175, 18790, 15360, 14126, and 8653  
 437 ¥/t, respectively. The domestic Mg ingot price fluctuates between 13,800 and 17,800  
 438 ¥/t during 2019 according to Tonhuashun finance (a Chinese financial website). It can  
 439 be seen that the current raw magnesium production industry in Fugu (S1) is vulnerable to  
 440 market fluctuations because of its meager profit. It indicates that only S1, S2 and S6 can  
 441 be profitable and economically competitive at the lowest magnesium price.

442 In Fugu, a large amount of waste semi-coke gas is produced due to the concentration  
 443 of the local coal chemical industry. Thus, the fuel is cheap or even free, and the fuel cost  
 444 of Mg ingots can be neglected in Fugu. But in other areas, fuel costs must be taken into  
 445 account if there is no cheap fuel gas. For S1, the cost of Mg ingots is primarily due to the  
 446 costs associated with the reductant, the reduction pots, the electricity, raw ores, and fuel.  
 447 Compared with S1, the average production cost of S2 only is reduced by about 750 ¥/t.  
 448 The average cost of S3 increases about 8800 ¥/t because of the costly aluminum  
 449 reductant and the extra fuel cost caused by the producer gas. The reduction in costs at S4  
 450 is mainly due to the free coke oven gas from the steelworks. Benefiting from the lower  
 451 fuel costs, S4's production cost is still considerably higher than that of S1. When  
 452 aluminum is introduced as the reductant in S3 and S4, the cost of magnesium ingots rise

453 sharply, and the average price exceeds the top of the market because of the high cost of  
 454 aluminum reductant. It indicates that the reductants takes a lion's share in the cost of the  
 455 aluminum process. As a result, even with free fuel, S3 and S4 are not economically  
 456 competitive. When the abandoned magnesite is reused, the cost of raw ores is roughly  
 457 halved. However, the average cost in S5 is still higher than in S1 and even higher than  
 458 the lowest Mg price, as the cost of fuel is not negligible and offset. The process will have  
 459 a price advantage when the fuel gas is freely provided, as in the case of S6. Therefore,  
 460 from the economic perspective, S6 is the best choice due to its low production cost, which  
 461 leads to a high economic profit.

462 In addition to the production costs of reduction pots, electricity, fuel, catalysts,  
 463 reductants, and raw ores, the environmental cost of the environmental burden of GHG  
 464 emissions is also considered in this study. The monetization of GHG emissions is  
 465 achieved through the carbon trading system, so the environmental burden of greenhouse  
 466 gas emissions can be directly shown in the form of economic costs. To combat climate  
 467 change and global warming, some countries, including China, are establishing carbon  
 468 trading systems aiming at reducing GHG emissions. The European Union Emission  
 469 Trading Scheme (EUETS), which is the first multi-national emissions trading system  
 470 around the world, was established by the EU in 2005 [40]. In 2011, the National  
 471 Development and Reform Commission of China approved Beijing, Tianjin, Shanghai,  
 472 Chongqing, Hubei, Guangdong, and Shenzhen to implement carbon emission trading  
 473 pilot work (NDRC, China, 2011). Based on this pilot experience, China has begun to  
 474 steadily establish a national carbon trading market since 2017 [41]. At present, China's  
 475 carbon trading market has been established and opened for trading.

476 Based on the trading data of the carbon market, the average cost of GHG emission  
 477 is 53 ¥/t. In the EU, the trading cost is 25 €/t (that is 191 ¥/t according to 7.65 of the  
 478 exchange rate). With the carbon trading costs included, the average Mg production costs  
 479 are shown in Fig. 7. The GHG emission level of S1 is taken as the baseline. When a  
 480 plant's GHG emissions exceed the baseline, it have to buy an additional carbon quota.  
 481 And when its emissions are below the baseline, it can sell its carbon quota.



483 Fig. 7. Production costs of the six scenarios considering the carbon cost.

484 The production costs of S2, S3, S4, S5, and S6 are 8124.5, 17815.9, 13126.8,  
485 14049.6 and 6570.7 ¥/t, respectively, considering the carbon price of the EU, and are  
486 8696.5, 18346.3, 14341.6, 14091.2 and 7704.3 ¥/t, respectively, based on China's  
487 carbon price. It is clear that the production cost varies greatly when taking into account  
488 the cost of carbon emissions. The production costs of all the alternative processes have  
489 reduced as a result of the reduction in GHG emissions.

490 Note that there's a significant cost reduction in S4 and S6 because of the great  
491 reduction in GHG emissions. It can be seen that the production cost of S5 is slightly  
492 reduced due to its limited GHG emission reduction. For S3, although it benefits from  
493 carbon trading, the production costs are still higher than the highest magnesium market  
494 price because the additional cost of reductant is not offset by the subsidies of carbon  
495 emissions reduction, even in high carbon price zone. Even using free and low carbon  
496 emissions fuel gasses, the price of S4 after the carbon subsidy is still higher than that of  
497 S2 and S6, indicating that the alumino-thermic method is not economically competitive  
498 compared to the silicon-thermic method. The carbon subsidies increases the economic  
499 competitiveness of S6, making it the cheapest option. Therefore, S6 is still the most  
500 economical option considering the environmental burden of GHG emissions.

501

## 502 4. Conclusion

503 This study evaluated the environmental and economic performance of the major  
504 prevailing metallic magnesium production processes, the Pidgeon process and five other  
505 alternative production processes through energy consumption, carbon emissions and  
506 economic characteristics in a view of life cycle. The data of energy consumption and  
507 GHG emission through the current Pidgeon process (in Fugu) are updated to  $6.38 \times 10^5$  MJ  
508 and 39.3 t CO<sub>2</sub>-eq., through fully relying on the domestic database. These data well  
509 reflected the actual level of domestic magnesium production technology and are of great  
510 significance for determining the initial carbon quota of domestic magnesium industry.

511 For the energy consumption of Pidgeon process, the fossil fuels (washed coal and  
512 semi-coke gas), and ferrosilicon contribute more than 95%. In descending order, the main  
513 contributions to the carbon emissions from the Pidgeon process are reductant production,  
514 fuel combustion, fuel production and carbonate decomposition. Energy conservation and  
515 emission reduction measures in the magnesium industry based on the Pidgeon process  
516 should focus on reductants and fuels.

517 Through the carbon trading markets in Europe and China, the environmental impacts  
518 of GHG emissions corresponding to the six scenarios are translated into their specific  
519 economic costs, which can be compared numerically. The evaluated case S6 has the  
520 lowest production costs, at 7704.3 and 6570.7 ¥/t, based on the Chinese and EU carbon

521 prices, respectively. It was demonstrated that the route of magnesium production with  
522 local abandoned magnesite and the redundant coke oven gas from the steelworks and the  
523 novel calcination technology has the best economic performance with the cited  
524 comprehensive considerations.

## 525 **CRedit authorship contribution statement**

526 **Xiaorui Huang:** Conceptualization, Data curation, Formal analysis, Investigation,  
527 Writing. **Zifu Xu:** Validation, Investigation. **Liangliang Fu:** Validation, Data curation.  
528 **Zhennan Han:** Validation. **Kun Zhao:** Validation. **Kangjun Wang:** Conceptualization,  
529 Funding acquisition. **Dingrong Bai:** Writing-review & editing. **Guangwen Xu:** Writing-  
530 review & editing, Supervision.

## 531 **Declaration of Competing Interest**

532 The authors declare that they have no known competing financial interests or personal  
533 relationships that could have appeared to influence the work reported in this paper.

## 534 **Acknowledgments**

535 The authors would like to gratefully acknowledge the online LCA platform  
536 WebLCA provided by IKE corporation and Sichuan University. This work is supported  
537 by the National Key R&D Program of China (No.2020YFC1909304).

538

## 539 **References**

- 540 [1] R. C. Ropp, "The Alkaline Earths as Metals," *Encyclopedia of the Alkaline Earth Compounds*,  
541 pp. 1–23, 2013, doi: 10.1016/b978-0-444-59550-8.00001-6.
- 542 [2] Z. Wang, "Application history and current situation of magnesium in aerospace," *World*  
543 *Nonferrous Metals*, vol. 09, pp. 68–69, 2010.
- 544 [3] J. Yin, "The development and prospect of magnesium industry in the world," *World*  
545 *Nonferrous Metals*, vol. 7, pp. 58–66, 2005.
- 546 [4] F. Cherubini, M. Raugei, and S. Ulgiati, "LCA of magnesium production. Technological  
547 overview and worldwide estimation of environmental burdens," *Resour Conserv Recycl*, vol.  
548 52, no. 8–9, pp. 1093–1100, 2008, doi: 10.1016/j.resconrec.2008.05.001.
- 549 [5] T. Xu, Y. Yang, X. Peng, J. Song, and F. Pan, "Overview of advancement and development trend  
550 on magnesium alloy," *Journal of Magnesium and Alloys*, vol. 7, no. 3, pp. 536–544, 2019, doi:



- 551 10.1016/j.jma.2019.08.001.
- 552 [6] J. Song, J. She, D. Chen, and F. Pan, "Latest research advances on magnesium and magnesium  
553 alloys worldwide," *Journal of Magnesium and Alloys*, vol. 8, no. 1, pp. 1–41, 2020, doi:  
554 10.1016/j.jma.2020.02.003.
- 555 [7] M. Hasan and L. Begum, "Semi-continuous casting of magnesium alloy AZ91 using a filtered  
556 melt delivery system," *Journal of Magnesium and Alloys*, vol. 3, no. 4, pp. 283–301, 2015, doi:  
557 10.1016/j.jma.2015.11.005.
- 558 [8] W. hui Liu, X. Liu, C. ping Tang, W. Yao, Y. Xiao, and X. he Liu, "Microstructure and texture  
559 evolution in LZ91 magnesium alloy during cold rolling," *Journal of Magnesium and Alloys*, vol.  
560 6, no. 1, pp. 77–82, 2018, doi: 10.1016/j.jma.2017.12.002.
- 561 [9] H. Liu *et al.*, "Microstructure and mechanical property of a high-strength Mg–10Gd–6Y–  
562 1.5Zn–0.5Zr alloy prepared by multi-pass equal channel angular pressing," *Journal of*  
563 *Magnesium and Alloys*, vol. 5, no. 2, pp. 231–237, 2017, doi: 10.1016/j.jma.2017.05.002.
- 564 [10] F. Abbassi, M. Srinivasan, C. Loganathan, R. Narayanasamy, and M. Gupta, "Experimental and  
565 numerical analyses of magnesium alloy hot workability," *Journal of Magnesium and Alloys*,  
566 vol. 4, no. 4, pp. 295–301, 2016, doi: 10.1016/j.jma.2016.10.004.
- 567 [11] S. Jayasathyakawin, M. Ravichandran, N. Baskar, C. Anand Chairman, and R. Balasundaram,  
568 "Mechanical properties and applications of Magnesium alloy – Review," *Mater Today Proc*,  
569 no. xxxx, 2020, doi: 10.1016/j.matpr.2020.01.255.
- 570 [12] Q. Lu, J. Chai, S. Wang, Z. G. Zhang, and X. C. Sun, "Potential energy conservation and CO2  
571 emissions reduction related to China's road transportation," *J Clean Prod*, vol. 245, no. 80, p.  
572 118892, 2020, doi: 10.1016/j.jclepro.2019.118892.
- 573 [13] W. Sun, X. Chen, and L. Wang, "Analysis of energy saving and emission reduction of vehicles  
574 using light weight materials," *Energy Procedia*, vol. 88, pp. 889–893, 2016, doi:  
575 10.1016/j.egypro.2016.06.106.
- 576 [14] N. R. Neelameggham, *Primary production of magnesium*. Woodhead Publishing Limited, 2013.  
577 doi: 10.1533/9780857097293.1.
- 578 [15] L. M. Pidgeon and J. A. King, "The vapour pressure of magnesium in the thermal reduction of  
579 MgO by ferrosilicon," *Discuss Faraday Soc*, vol. 4, pp. 197–206, 1948, doi:  
580 10.1039/DF9480400197.
- 581 [16] W. A. A. L.M. Pidgeon, "Thermal production of magnesium-pilot-plant studies on the retort  
582 ferrosilicon process," *Trans. Am. Inst. Min. Met. Eng.*, vol. 159, pp. 315–352, 1944.
- 583 [17] C. Wang, S. Zhang, and L. Guo, "Investigation on the effective thermal conductivity of typical  
584 Pidgeon process briquette with a combined model," *Int J Heat Mass Transf*, vol. 115, pp.  
585 1348–1358, 2017, doi: 10.1016/j.ijheatmasstransfer.2017.08.064.

- 586 [18] H. Liu, Y. Dai, Y. Tian, T. Qu, and Q. Yu, "The environmental issues of the magnesium produced  
587 in Chian using the Pidgeon process," *Light Metals*, vol. 11, pp. 43–48, 2010.
- 588 [19] P. An *et al.*, "Energy-saving strategy for a transport bed flash calcination process applied to  
589 magnesite," *Carbon Resources Conversion*, vol. 4, pp. 122–131, Jan. 2021, doi:  
590 10.1016/j.crcon.2021.03.004.
- 591 [20] N. Xiong, Y. Tian, B. Yang, B. qiang Xu, T. Dai, and Y. nian Dai, "Results of recent investigations  
592 of magnesia carbothermal reduction in vacuum," *Vacuum*, vol. 160, pp. 213–225, 2019, doi:  
593 10.1016/j.vacuum.2018.11.007.
- 594 [21] P. Deng, Y. Liu, W. Yao, and H. Ma, "Production of Primary Magnesium by the Aluminothermic  
595 Reduction of Magnesia Extracted from Dolomite Ore," *Materials Science Forum*, vol. 788, pp.  
596 28–33, Apr. 2014, doi: 10.4028/www.scientific.net/MSF.788.28.
- 597 [22] J. Li, X. Ma, H. Liu, and X. Zhang, "Life cycle assessment and economic analysis of methanol  
598 production from coke oven gas compared with coal and natural gas routes," *J Clean Prod*, vol.  
599 185, pp. 299–308, 2018, doi: 10.1016/j.jclepro.2018.02.100.
- 600 [23] D. Huber, D. Costa, A. Felice, P. Valkering, T. Coosemans, and M. Messagie, "Decentralized  
601 energy in flexible energy system: Life cycle environmental impacts in Belgium," *Science of The  
602 Total Environment*, vol. 886, p. 163882, 2023, doi:  
603 <https://doi.org/10.1016/j.scitotenv.2023.163882>.
- 604 [24] P. Yue *et al.*, "Life cycle and economic analysis of chemicals production via electrolytic  
605 (bi)carbonate and gaseous CO<sub>2</sub> conversion," *Appl Energy*, vol. 304, Dec. 2021, doi:  
606 10.1016/j.apenergy.2021.117768.
- 607 [25] A. Sarrion, E. Medina-Martos, D. Iribarren, E. Diaz, A. F. Mohedano, and J. Dufour, "Life cycle  
608 assessment of a novel strategy based on hydrothermal carbonization for nutrient and energy  
609 recovery from food waste," *Science of The Total Environment*, vol. 878, p. 163104, 2023, doi:  
610 <https://doi.org/10.1016/j.scitotenv.2023.163104>.
- 611 [26] Z. Zhu and C. Lu, "Life cycle assessment of shared electric bicycle on greenhouse gas emissions  
612 in China," *Science of The Total Environment*, vol. 860, p. 160546, 2023, doi:  
613 <https://doi.org/10.1016/j.scitotenv.2022.160546>.
- 614 [27] F. Gao, Z. ren Nie, Z. hong Wang, X. zheng Gong, and T. yong Zuo, "Assessing environmental  
615 impact of magnesium production using Pidgeon process in China," *Transactions of  
616 Nonferrous Metals Society of China*, vol. 18, no. 3, pp. 749–754, 2008, doi: 10.1016/S1003-  
617 6326(08)60129-6.
- 618 [28] R. S. and K. P., "A Comparison of the Greenhouse Impacts of Magnesium Produced By  
619 Electrolytic and Pidgeon Processes," *Essential Readings in Magnesium Technology. Springer,  
620 Cham*, pp. 169–174, 2016, doi: [https://doi.org/10.1007/978-3-319-48099-2\\_28](https://doi.org/10.1007/978-3-319-48099-2_28).
- 621 [29] H. Li, W. Zhang, Q. Li, and B. Chen, "Updated CO<sub>2</sub> emission from Mg production by Pidgeon

- 622 process: Implications for automotive application life cycle," *Resour Conserv Recycl*, vol. 100,  
623 pp. 41–48, 2015, doi: 10.1016/j.resconrec.2015.04.008.
- 624 [30] S. Ehrenberger, "Assessment of Magnesium Components in Vehicle," no. April 2014, 2013.
- 625 [31] S. Ramakrishnan and P. Koltun, "Global warming impact of the magnesium produced in China  
626 using the Pidgeon process," *Resour Conserv Recycl*, vol. 42, no. 1, pp. 49–64, 2004, doi:  
627 10.1016/j.resconrec.2004.02.003.
- 628 [32] D. X. Fu, N. X. Feng, Y. W. Wang, J. P. Peng, and Y. Z. Di, "Kinetics of extracting magnesium  
629 from mixture of calcined magnesite and calcined dolomite by vacuum aluminothermic  
630 reduction," *Transactions of Nonferrous Metals Society of China (English Edition)*, vol. 24, no.  
631 3, pp. 839–847, 2014, doi: 10.1016/S1003-6326(14)63133-2.
- 632 [33] W. Hu, N. Feng, Y. Wang, and Z. Wang, "Magnesium production by vacuum aluminothermic  
633 reduction of a mixture of calcined dolomite and calcined magnesite," *Magnesium Technology*,  
634 pp. 121–122, 2011.
- 635 [34] Y. Tian *et al.*, "Comparative evaluation of energy and resource consumption for vacuum  
636 carbothermal reduction and Pidgeon process used in magnesium production," *Journal of*  
637 *Magnesium and Alloys*, 2020, doi: 10.1016/j.jma.2020.09.024.
- 638 [35] V. T. Luong, R. Amal, J. A. Scott, S. Ehrenberger, and T. Tran, "A comparison of carbon  
639 footprints of magnesium oxide and magnesium hydroxide produced from conventional  
640 processes," *J Clean Prod*, vol. 202, pp. 1035–1044, 2018, doi: 10.1016/j.jclepro.2018.08.225.
- 641 [36] M. Hecheng *et al.*, "Research on the method and practice of life cycle impact assessment in  
642 China", doi: 10.12153/j.issn.1674-991X.20210544.
- 643 [37] F. ; Verones, A. D. Henderson, A. ; Laurent, B. ; Ridoutt, C. ; Ugaya, and S. Hellweg, "LCIA  
644 framework and modelling guidance," UNEP, 2016. [Online]. Available:  
645 [www.lifecycleinitiative.org](http://www.lifecycleinitiative.org)
- 646 [38] W. H.-T. Liu Xia-Lu, "Method and basic model for development of Chinese reference life cycle  
647 database," *Acta Science Circumstantiae*, vol. 30, no. 10, pp. 2136–2144, 2010.
- 648 [39] S. Ehrenberger, "Carbon Footprint of Magnesium Production and its Use in Transport  
649 Applications." [Online]. Available: <https://www.researchgate.net/publication/349254199>
- 650 [40] Y. P. Liu, J. F. Guo, and Y. Fan, "A big data study on emitting companies' performance in the  
651 first two phases of the European Union Emission Trading Scheme," *J Clean Prod*, vol. 142, pp.  
652 1028–1043, 2017, doi: 10.1016/j.jclepro.2016.05.121.
- 653 [41] F. Wen, N. Wu, and X. Gong, "China's carbon emissions trading and stock returns," *Energy*  
654 *Econ*, vol. 86, p. 104627, 2020, doi: 10.1016/j.eneco.2019.104627.

656 **Website References**

657 MIIT, PRC, 2019. Operation of magnesium industry in 2018.

658 <http://www.miit.gov.cn/n1146285/n1146352/n3054355/n3057569/n3057572/c6666>  
659 128/content.html.

660 Fugu Bureau of Statistics, 2014. Circular economy promotes green transformation and  
661 development . <http://www.fg.gov.cn/info/1133/14594.htm>

662 IMA , 2012. IMA Award Winners

663 Spotlight Magnesium Innovation. [https://cdn.ymaws.com/intlmag.site-](https://cdn.ymaws.com/intlmag.site-ym.com/resource/resmgr/docs/recycling/MgShowcase_summer2012FINAL.pdf)  
664 [ym.com/resource/resmgr/docs/recycling/MgShowcase\\_summer2012FINAL.pdf](https://cdn.ymaws.com/intlmag.site-ym.com/resource/resmgr/docs/recycling/MgShowcase_summer2012FINAL.pdf).

665 NDRC, China, 2011. Circular of the general office of the national development and  
666 Reform Commission on the pilot work of carbon emission trading.

667 [https://www.ndrc.gov.cn/xxgk/zcfb/](https://www.ndrc.gov.cn/xxgk/zcfb/tz/201201/t20120113_964370.html) tz/201201/t20120113\_964370.html

668 China carbon emissions trading website. <http://www.tanpaifang.com>

## Declaration of interests

Guangwen Xu is an editor-in-chief for Carbon Resources Conversion and was not involved in the editorial review or the decision to publish this article. All authors declare that there are no competing interests.

## Highlights

- First life cycle assessment of the current magnesium production process based

native database in China.

- Life cycle assessment is used to determine the potential and viable processes in magnesium industry.
- GHG emissions from the production process are monetized through the carbon emission trading scheme.
- GHG emissions and energy consumption results of the current magnesium production process in China are updated.
- The magnesium production process based on the fluidized bed is verified the best choice for Liaoning by LCA.